ASTROBIOLOGY
Volume 8, Number 3, 2008

DOI: 10.1089/ast.2006.0092

Research Paper

A Facility for Long-Term Mars Simulation Experiments: The Mars Environmental Simulation Chamber (MESCH)

Lars Liengaard Jensen,[1] Jonathan Merrison,[2] Aviaja Anna Hansen,[1] Karina Aarup Mikkelsen,[1] Tommy Kristoffersen,[1] Per Nørnberg,[3] Bente Aagaard Lomstein,[1] and Kai Finster[1]

Abstract

We describe the design, construction, and pilot operation of a Mars simulation facility comprised of a cryogenic environmental chamber, an atmospheric gas analyzer, and a xenon/mercury discharge source for UV generation. The Mars Environmental Simulation Chamber (MESCH) consists of a double-walled cylindrical chamber. The double wall provides a cooling mantle through which liquid N_2 can be circulated. A load-lock system that consists of a small pressure-exchange chamber, which can be evacuated, allows for the exchange of samples without changing the chamber environment. Fitted within the MESCH is a carousel, which holds up to 10 steel sample tubes. Rotation of the carousel is controlled by an external motor. Each sample in the carousel can be placed at any desired position. Environmental data, such as temperature, pressure, and UV exposure time, are computer logged and used in automated feedback mechanisms, enabling a wide variety of experiments that include time series. Tests of the simulation facility have successfully demonstrated its ability to produce temperature cycles and maintain low temperature (down to −140°C), low atmospheric pressure (5–10 mbar), and a gas composition like that of Mars during long-term experiments. Key Words: Mars simulation facility—UV radiation—Environmental incubation—Artificial atmosphere—Low temperature—Low pressure. Astrobiology 8, 537–548.

1. Introduction

In recent years, there has been an increase in the number of scientific missions to Mars and studies on the effects of martian environmental conditions on terrestrial life (Table 1) [Brack, 2000; Squyres, *et al.*, 2004a, 2004b; UALPL, 2008 (see http://phoenix.lpl.arizona.edu)]. Due to the availability of more accurate and detailed information about the atmospheric and surface conditions on Mars, it is now possible to create proxy-martian conditions in the laboratory and subject samples to these conditions. The effects of martian environmental conditions on terrestrial microorganisms have been studied in simulation experiments for 2 major reasons: first, to evaluate the risk of forward contamination of Mars with terrestrial microbiota by way of Mars missions; and, second, to investigate the suitability of the martian environment for supporting life.

When simulating martian conditions, the most important parameters are high ultraviolet (UV) radiation (200–400 nm), low pressure (6–10 mbar), specific atmospheric composition (95% CO_2, 3% N_2, 1.5% Ar, 0.1% O_2, and 0.01% CO by volume), and low temperatures in the dark (−20°C to −80°C). The temperature on Mars varies on a geographical, seasonal, and diurnal scale; and surface temperatures can locally exceed 20°C during the day (Kieffer *et al.*, 1992). Furthermore, the study and control of humidity is important in the simulation of martian conditions. Water can be a source for reactive chemicals (UV induced), mediate the transport of soluble chemicals, and affect heat dissipation within soil (Lobitz *et al.*, 2001).

Facilities for simulation of martian conditions have evolved along with increased insight into the abiotic conditions on Mars, starting with very simple anoxic systems to highly sophisticated simulation chambers (Table 1). The con-

[1]Department of Biological Sciences, Section for Microbiology, [2]Department of Physics and Astronomy, and [3]Department of Earth Sciences, University of Aarhus, Aarhus, Denmark.

Table 1. Incubation Conditions Applied in Studies on the Biological Response to Simulated Martian Conditions

Year	Incubation method	Temperature (°C)	Pressure (mbar)	Atmospheric composition (%) CO_2	N_2	Ar	C_2	Solar radiation (nm)	lamp	Water addition (%)	Nutrients present[a]	Reference
Present Mars	—	−123 to +25	6.7–9.9	95.3	2.7	1.6	0.13	>200	—	—	—	
1958	Anaerobic Jar	−25/25†	87	—	100	—	—	—	—	1	—	Fulton, 1958
	Anaerobic Jar	−22/25†	72	—	100	—	—	—	—	1	—	Kooistra *et al.*, 1958
1959	Anaerobic Jar	−25/25†	87	—	100	—	—	—	—	1	—	Davis and Fulton, 1959
1962	Anoxic tubes	−25/25†	~0/87	—	100	—	—	—	—	—	—	Hawrylewicz *et al.*, 1962
1963	Anaerobic Jar	−60/20†	100	5	95	—	—	254[b]	Mercury	—	—	Packer *et al.*, 1963
	Anoxic tubes	−75/25†	1013[c]	—	100	—	—	—	—	100	+	Young *et al.*, 1963
1964	Anoxic tubes	−60/26†	113	2.2	93.8	4	—	—	—	0.5	+	Hagen *et al.*, 1964
1965	Anoxic tubes	−65/25†	113	2.2	93.8	4	—	—	—	<1	+	Hawrylewicz *et al.*, 1965
	Mars facility	−60/25†	100	0.25	95.5	0.25	—	200–2500	Xenon	—	—	Zhukova and Kondratyev, 1965
1967	Anoxic tubes	−65/28†	113	2.2	93.8	4	0–2%	—	—	+/−	1%	Hagen *et al.*, 1967
	Tubes	−60/25†	1013[c]	0.03[c]	78.1[c]	0.93[c]	20.9[c]	254	Mercury	100	+	Imshenetsky *et al.*, 1967
1968	Mars facility	−64/28†	100	—	100	—	—	240–280	Mercury	$\alpha_w = 0.49$	—	Belikova *et al.*, 1968
	Anoxic tubes	−65/30†	10–40	37–100	13–27	21–30	—	—	—	+	1%	Hawrylewicz *et al.*, 1968
1969	Mars facility	18–20†	7.1–60	—	99	—	≤1	—	—	100	0.98	Lozina-Lozinsky and Bychenkova, 1969
1970	Mars facility	−65/30†	20	67	30	3	—	200–300	Mercury	1–2	—	Hagen *et al.*, 1970
1971	Mars facility	−60/25†	8	70	25	5	—	200–2500	Xenon	<1	—	Green *et al.*, 1971
	Anoxic tubes	−25/25†	13	99	—	—	—	—	—	5	1%	Lozina-Lozinsky *et al.*, 1971
1973	Anoxic tubes	−60/28†	7	80	—	20	—	—	—	(+)[d]	+	Imshenetsky *et al.*, 1973
1974	—	−65/25†	7	80	—	20	—	—	—	—	—	Foster and Winans, 1974
1978	Anoxic tubes	−65/24†	7	99.9	—	—	0.01	—	—	—	—	Foster *et al.*, 1978
1979	Tubes	−10 to +25‡	0.001	—	100	—	(+/−)[e]	200–300	Mercury/xenon	—	—	Oro and Holzer, 1979
1984	Mars facility	−80/20†	7–9	95	2–3	1–2	<0.4	254	Mercury	<0.4	—	Imshenetskii *et al.*, 1984
1992	Anoxic tubes	−70†	13	95.52	2.73	1.62	0.13	—	—	4/50	—	Moll and Vestal, 1992
1995	Mars facility	−160 to +50‡	0.001	95.46	2.7	1.6	0.17	115–400	Hydrogen	—	—	Koike *et al.*, 1995
1996	Mars facility	60‡	10	95.46	2.7	1.6	0.17	115–400	Hydrogen	—	—	Koike *et al.*, 1996
1997	Mars facility	Room temp	100	95.59	—	4.21	0.11	210–710	Xenon	—	—	Stoker and Bullock, 1997
1998	Tubes	−23 to +10‡	1013[c]	—	—	—	—	—	—	100	—	McDonald *et al.*, 1998
2000	—	25	1013[c]	0.03[c]	78.1[c]	0.93[c]	20.9[c]	200–400	Deuterium	—	—	Mancinelli and Klovstad, 2000

2003	Mars facility	−10[†]	8.5	95.3	2.7	1.7	0.2	200–2500	Xenon	—	—	Schuerger *et al.*, 2003
	Mars facility	−60[†]	6	98	—	—	—	—	—	2/100	—	Stan-Lotter *et al.*, 2003
2005	Mars facility	−10[†]	8.5	100	—	—	—	200–2500	Xenon	—	—	Cockell *et al.*, 2005
												Schuerger *et al.*, 2005
	Mars facility	−95 to +12[‡]	9–13	77.5	8.7	—	1.3	200–2500	Xenon-mercury	—	—	Hansen *et al.*, 2005
	Mars facility	20[‡]	12.5	100	—	—	—	—	—	—	—	Nicholson and Schuerger, 2005
	Mars facility	Room temp	4×10^6	—	—	—	—	120–180	Hydrogen	—	—	ten Kate *et al.*, 2005
2006	Jars and Beakers	−35	833	0.03[c]	78.1[c]	0.93[c]	20.9[c]	200–400	Deuterium	—	—	Diaz and Schulze-Makuch, 2006
	Mars facility	−75 to +20	6	95.3	—	—	—	—	—	10^{-3}mbar	—	Morozova *et al.*, 2006
	Mars facility	23	1013	0.03[c]	78.1[c]	0.93[c]	20.9[c]	200–400	Xenon	—	—	Schuerger *et al.*, 2006
	Mars facility	26	7.1	99.9	—	—	—	200–400	Xenon	—	—	Tauscher *et al.*, 2006
	Mars facility	−63 and room temperature	10^{-7} and 7	99.9	—	—	—	190–325	Deuterium	—	—	ten Kate *et al.*, 2006

Included for reference are the conditions at the surface of present-day Mars. Only a selection of the reported experiments is included.
+, Water or nutrients were added, no indication of amount.
+/−, A compound was present in some experiments and absent in others, no indication of amount.
−, Not included in the simulation experiment.
[†]Diurnal cycles between the 2 temperatures.
[‡]Constant temperature.
[a]+, The organisms were incubated in their growth media.
[b]Minor part of the experiment.
[c]Earth conditions.
[d]Water was present in the solidified growth medium.
[e]Oxygen of unknown pressure was included in some of the experiments.

ditions provided in the early experiments could hardly be called martian; they resembled more traditional anoxic incubations that use anoxic tubes or anaerobic jars. The only modification compared to conventional anoxic incubations of microorganisms was the temperature cycles achieved by alternately moving the samples from a freezer to room temperature in the laboratory.

Zhukova and Kondratyev (1965) were the first to use a simulation chamber that was designed for the incubation of pure cultures of bacteria and fungi under conditions that simultaneously simulated martian temperatures, pressure, atmospheric composition, and solar radiation. Despite the obvious benefits of simulating the physical parameters simultaneously, only 6 out of 26 studies reported between 1958 and 1990 used simulation chambers (Table 1) (Zhukova and Kondratyev, 1965; Belikova *et al.*, 1968; Lozina-Lozinsky and Bychenkova, 1969; Hagen *et al.*, 1970; Green *et al.*, 1971; Imshenetskii *et al.*, 1984). In the same period, only 8 studies included UV radiation, where 5 of these used simulation chambers for their investigations (Packer *et al.*, 1963; Zhukova and Kondratyev, 1965; Imshenetsky *et al.*, 1967; Belikova *et al.*, 1968; Hagen *et al.*, 1970; Green *et al.*, 1971; Oro and Holzer, 1979; Imshenetskii *et al.*, 1984). Today, most studies use simulation chambers and include UV radiation (Table 1), which has been identified as extremely harmful to microorganisms (*e.g.*, Mancinelli and Klovstad, 2000; Schuerger *et al.*, 2003).

The nature of the UV radiation applied in the different studies has generally been poorly defined in terms of either radiation spectrum or intensity dose. However, the type of UV lamps applied in the different studies can be used to identify whether the simulated UV radiation corresponds to the current martian UV models. In total, 8 studies have used xenon lamps to generate UV light (Table 1) (Zhukova and Kondratyev, 1965; Green *et al.*, 1971; Oro and Holzer, 1979; Stoker and Bullock, 1997; Schuerger *et al.*, 2003; Cockell *et al.*, 2005; Schuerger *et al.*, 2005, 2006; Tauscher *et al.*, 2006). UV light generated from xenon lamps is now considered to simulate the present martian UV environment most accurately in terms of the fluence rates of the different wavelengths (Schuerger *et al.*, 2003). Other studies have used mercury lamps (Packer *et al.*, 1963; Imshenetsky *et al.*, 1967; Belikova *et al.*, 1968; Hagen *et al.*, 1970; Oro and Holzer, 1979; Imshenetskii *et al.*, 1984), a combination of xenon/mercury lamps (Hansen *et al.*, 2005), deuterium lamps, or hydrogen lamps (Koike *et al.*, 1995, 1996; Mancinelli and Klovstad, 2000; ten Kate *et al.*, 2005). All these light sources have a relatively higher fluence rate in the UVC region (200–280 nm) than found on Mars. Therefore, these lamps produce an environment that is more harmful than the *in situ* martian light climate. Furthermore, the spectra of mercury, deuterium, and hydrogen lamps are relatively narrow and do not include the full spectrum of visible (VIS) and infrared (IR) light (700–2500 nm), as do xenon lamps and the incident solar radiation on Mars. Due to these differences in UV light simulations, there has been increased focus in designing UV light sources, which have a spectrum and irradiance levels equiv-

TABLE 2. A SELECTION OF MARS SIMULATION FACILITIES ON WHICH INFORMATION HAS BEEN PUBLISHED IN PEER-REVIEWED JOURNALS

	Applications/properties of the simulator	*Reference*
Mars Simulator, DLR, Germany	Physical, chemical and biological experiments under simulated martian conditions	Seidensticker *et al.*, 1995
EXOCAM, Service d'Aéronomie, France	Physical-chemical interactions between the atmosphere and the surface and subsurface in martian conditions	Rannou *et al.*, 2001
ANDROMEDA, Arkansas-Oklahoma Center for Space and Planetary Sciences, USA	Simulation of conditions in space, on asteroids, comet nuclei, and on Mars on the meter scale and surface and subsurface	Sears *et al.*, 2002
Combined atmospheric simulation chamber and solar simulator ESTEC, The Netherlands	Studying the combined effects of UV photoprocessing, atmospheric conditions, and the presence/absence of oxidizing agents on organic molecules	ten Kate *et al.*, 2003
SURFRESIDE Raymond and Beverley Sackler Laboratory, The Netherlands	Studying surface processes under pseudo-interstellar conditions on and in icy films	Fraser and van Dishoeck, 2003
Mars Simulation Chamber Kennedy Space Center, USA	Studying the effect of simulated martian conditions on bacterial monolayers	Schuerger *et al.*, 2003
Mars Simulation Chamber Space Research Institute, Austria	Survival experiments with halophilic archaea	Stan-Lotter *et al.*, 2003
Mars brines experimental apparatus, Department of Space Studies, Boulder, USA	Simulation of martian aqueous geochemistry	Bullock *et al.*, 2004
S.A.M. (Simulatore di Ambiente Marziano), Department of Astronomy, Padua, Italy	Bacterial cells, contained in capsules, will be exposed to thermal cycles simulating diurnal and seasonal martian cycles	Galetta *et al.*, 2006
Space simulator, Centro de Astrobiología, Madrid, Spain	A chamber capable of reproducing atmospheric composition, surface termperatures, and light climate for most planetary objects	Mateao-Martí *et al.*, 2006

alent to those found on Mars (Zill *et al.*, 1979; Schuerger *et al.*, 2003; Kolb *et al.*, 2005).

Apart from studies on the effect of martian conditions on biological material, simulation experiments have addressed issues in (geo)physics (*e.g.*, Merrison *et al.*, 2004) and (geo)chemistry (*e.g.*, Hubbard *et al.*, 1971; Moore and Bullock, 1999; Bullock *et al.*, 2004; Gontareva, 2005; Moore and Sears, 2006).

In recent years, sophisticated multi-purpose space simulators have been constructed and, in some cases, presented in peer-reviewed journals (Table 2). These chambers allow for the testing of material that will be included on missions to Mars or in biological experiments under proxy-martian conditions.

Here, we present a description and data on the properties of a Mars Environmental Simulation Chamber (MESCH) designed to reproduce the environmental conditions on Mars, specifically the near-surface region (*i.e.*, the uppermost few cm), with a special focus on temperature and light climate.

2. Design of the Mars Environmental Simulation Chamber

2.1. Mechanical design of the MESCH

The MESCH consists of a double-walled cylindrical chamber (3 mm 304 stainless steel) that has an internal diameter of 313 mm and an internal height of 396 mm (Fig. 1), which results in an internal volume of approximately 30 L. The double wall serves as a cooling mantle through which liquid N_2 can be circulated. The cooling mantle has 8 internal baffles, which ensure a uniform distribution of N_2 for the cooling of the chamber. The double wall contains an inspection window that enables observation of the samples during incubation and an access port for a Pirani pressure sensor (Pfeiffer PCR-260, Pfeiffer Vacuum GmbH, Asslar, Germany). To reduce heat transfer from the surroundings, the chamber is wrapped in multiple layers of super-insulating material (Cryogenic Insulation, Jehier Group, Hutchinson, Paris, France). Low pressure ($\sim 10^{-3}$ mbar) is achieved by pumping with a rotary vane vacuum pump (Edwards RV 5, BOC Edwards, West Sussex, United Kingdom) before the introduction of a gas mixture to create a martian atmosphere.

A 100 mm diameter quartz glass window is positioned in the lid (top) of the MESCH, which permits exposure of a sample to UV radiation via an angled mirror (Fig. 1). A load-lock system on the MESCH lid allows for the exchange of samples without changing the chamber environment. This load-lock system consists of a small pressure-exchange chamber (length: 500 mm; diameter: 70 mm), which can be evacuated without interrupting ongoing experiments. The

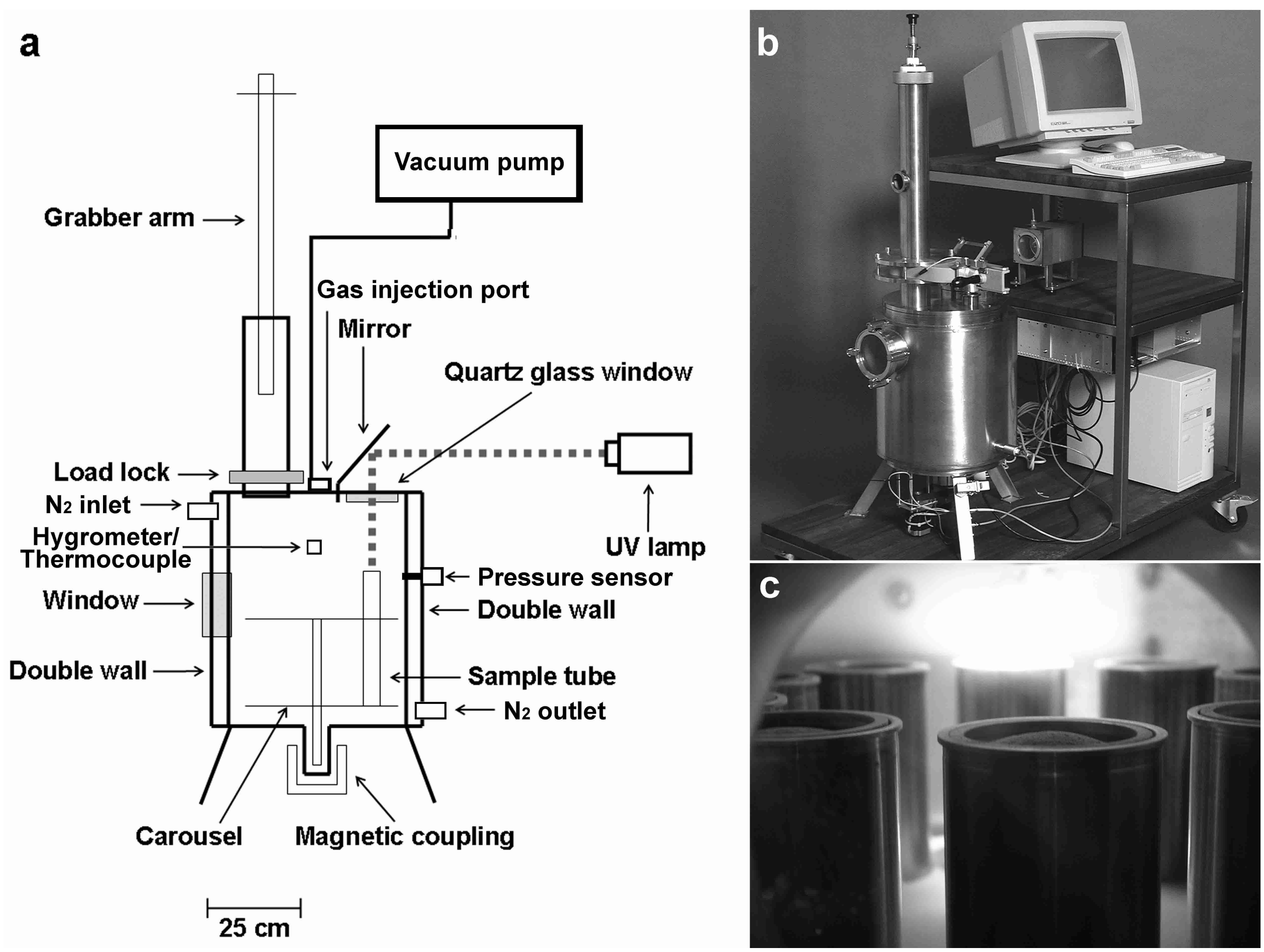

FIG. 1. (**a**) Schematic drawing of the Mars Environmental Simulation Chamber (MESCH) showing the double wall and the light path of the UV solar simulation source. (**b**) Photograph of the MESCH. (**c**) photograph of soil samples within the MESCH (one of which is being irradiated).

exchange chamber is connected to the main chamber via a Viton® sealed vacuum valve. A 900 mm long rod with a sample grip arm is used to insert and extract sample tubes remotely from the MESCH (Fig. 1).

Within the chamber there is a carousel that can hold 10 steel sample tubes. The carousel can be remotely rotated to position a sample either under the UV discharge source, the load-lock system, or at any desired position. In this way, controlled (light/heat) exposures can be performed in order to simulate diurnal cycling. The carousel is rotated by a stepper motor (JVL Industri MST-232B02, Birkerød, Denmark) controlled by a computer through a controller unit (JVL Industri SMC-24, Birkerød, Denmark). The stepper motor is connected to the carousel drive shaft via a magnetic coupling (Minex SA 46/6, KTR GmbH, Michigan City, Indiana, USA). A position sensor (Vishay RS-601, Proton Electronic components, Wroclaw, Poland) is connected to the stepper-motor drive shaft, which allows feedback of the carousel position to the computer. Data on pressure, temperature, UV solar simulation source intensity, humidity, sample position, and sample exposure are acquired by a computer using a program written in LabView (National Instruments, Austin, Texas, USA).

A Honeywell polymer film humidity sensor (Honeywell HIH-3602C, Honeywell, Minneapolis, USA) is used to monitor the relative humidity (water content) inside the MESCH. Similarly, an inbuilt platinum (film) thermistor is used for control of the MESCH temperature (cooling). The humidity/temperature sensor is attached to the inner chamber wall slightly above the liquid N_2 inlet. The advantage of this sensor is its insensitivity to atmospheric pressure. The MESCH temperature is controlled by the computer via a feedback system that activates and inactivates a solenoid valve between 2 selected temperatures. The valve is connected to a pressurized 160 L liquid N_2 tank. Figure 2 shows a schematic diagram of the inputs, outputs, and feedback mechanisms fitted to the system.

Special glass cylinders (length: 30 cm; internal diameter: 4 cm) have been constructed for incubation of soil samples in the MESCH. These glass cylinders are fitted with Teflon® stoppers to support the sample at a desired height during the incubation. Each glass cylinder is inserted into a steel tube (3 mm 304 stainless steel) to ensure that samples are only exposed to UV at the surface. If required, other types of sample containers can be mounted in the carousel.

2.2. UV solar simulation source (xenon/mercury discharge lamp)

Simulation of martian UV irradiance levels is achieved with the use of a 150 W mercury xenon lamp (Hamamatsu Photonics L2482, Hamamatsu Photonics Systems, Shizuoka, Japan). The lamp can be operated at different output levels, depending on the experimental requirements. Collimation was used such that only a single sample was exposed at one time. This exposure area was of the order of 50 mm wide (comparable to the sample diameter of 40 mm). The heat generated at the sample by the lamp is controllable in the range 200–600 W m^{-2}, which is comparable to the solar radiation influx on Mars, which has a maximum of 589 W m^{-2} (Kieffer *et al.*, 1992). Calibration of the lamp was performed by way of a photochemical process (actinometry), in which a photo-sensitive solution was used to determine the absolute UV photon flux (Bunce, 1987). The calibration measurement was performed with band-pass filters (10 nm width) at wavelengths of 239 nm, 281 nm, and 365 nm. The resultant radiation intensities were 0.21, 0.19, and 0.55 W m^{-2} nm^{-1}, respectively. During calibration and operation, care was taken to ensure a uniform illumination of the sample.

Direct measurements of the average UV flux on Mars have not been made. However, based on model calculations of the solar flux at the surface of Mars (Patel *et al.*, 2004), a value of 5.94×10^{-3} W m^{-2} nm^{-1} was obtained by averaging over a martian year and day at 11.6°N for a wavelength of 239 nm (M. Patel, personal communication). Compared to this value, the intensity of our lamp was ~35 times higher than the averaged UV flux (at 239 nm) at the surface of Mars. The optical spectrum of the lamp has been measured directly,

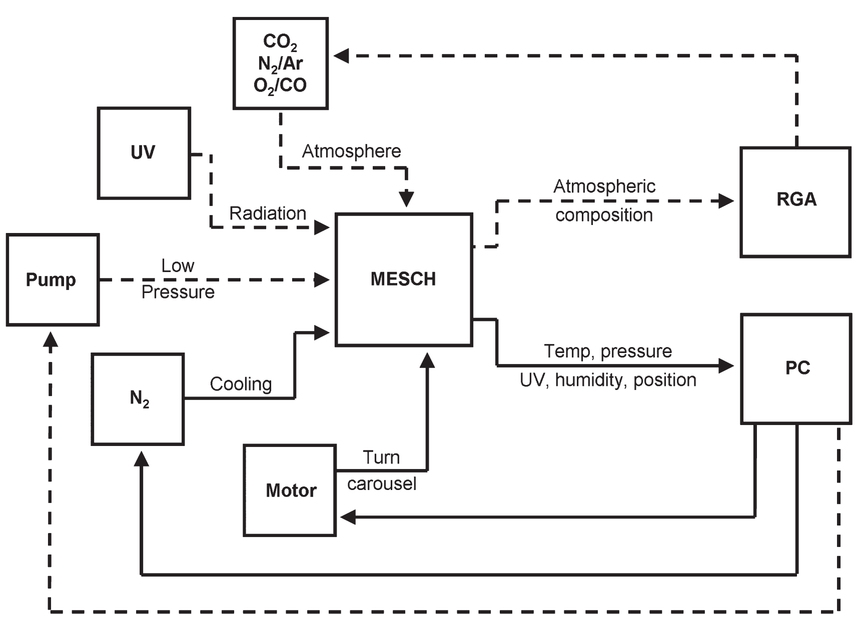

FIG. 2. Schematic drawing of the input and output systems of the MESCH. Solid arrows indicate automated feedback mechanisms controlled by the PC. Dashed arrows indicate manually controlled processes. RGA, Residual Gas Analyzer.

within the chamber, with the use of an AvaSpec-2048 (Avantes, Eerbeek, the Netherlands) irradiance spectrometer with a 300 lines/mm grating, fiber optical attachment, and an optical diffuser at the entrance. The spectrum is shown in Fig. 3 between the wavelengths of 230 nm and 1100 nm. Reasonable agreement is obtained between the absolute calibration and the irradiance values measured by way of the spectrometer. Comparison may also be made to the spectrum of the lamp obtained from the manufacturer's website (www.hamamatsu.co.uk).

It should be noted that Kolb *et al*. (2005) recently developed a solar simulation lamp that more accurately reproduces the spectrum and intensity in the martian UV range. The lamp used in our simulation system can be exchanged with any other type of lamp or radiation source if a different spectral composition and intensity are desired.

3. Testing and Calibration

3.1. Composition and control of the MESCH atmosphere

A martian atmosphere is produced by evacuating the MESCH to 10^{-3} mbar and refilling it in a stepwise procedure, whereby 0.45 mbar of a mixture of the minor gas constituents (60% N_2, 35% Ar, 3% O_2, and 2% CO) are first injected into the MESCH, and then CO_2 is injected in to produce a final pressure of 8.55 mbar with a resulting final gas composition of ~95% CO_2, 3% N_2, 1.5% Ar, 0.1% O_2, and 0.01% CO. The composition of the simulated atmosphere is monitored with a residual gas analyzer (Microvision plus RGA, MKS Instruments, USA).

Four key mass/charge components were selected for use in these experiments: CO_2^+ ($m/e = 44$), Ar^+ (40), O_2^+ (32), and H_2O^+ (18). By measuring the abundance of these 4 molecular components, we were able to establish important properties of the gas mixture, specifically: CO_2 concentration, the amount of added trace gas (Ar concentration), atmospheric gas leakage (O_2 concentration), and the absolute water vapor content (humidity). Though this water vapor determination was of only limited accuracy, it could be used for comparison with the *in situ* measurement of the relative humidity (Section 3.3).

Leak tests on the chamber were carried out in 2 ways: (1) Leak testing with helium while evacuating the MESCH and (2) Observation of pressure changes during a 9-day incubation of a sand sample in the MESCH. In the first leak test, the MESCH was evacuated to $\sim 10^{-5}$ mbar with a turbopump connected to a helium detector. Helium was flushed onto flanges, valves, and connectors on the outside of the MESCH. In case of leaks, helium would diffuse into the MESCH and be detected by the helium detector. This test revealed no leaks in the MESCH at the resolution of the helium detector. In the second leak test, a 9-day pressure experiment was performed in the MESCH, which was operated with a pure CO_2 atmosphere at 7 mbar and a preset wall temperature of $-50°C$. During the experiment, a freeze-dried sand sample was present in the carousel, and the UV lamp was switched on. By the end of the experiment, there had been a minor pressure increase of 0.1 ± 0.05 mbar, equivalent to 0.011 mbar day^{-1}. This pressure increase was probably caused by outgassing of residual water from the sand sample. Since the mean pressure on Mars is 6.4 ± 2.4 mbar, the pressure increase observed in this experiment is equivalent to <5% of mean martian atmospheric pressure in a month-long experiment. This is within the pressure variations observed on Mars. Hence, the MESCH is capable of maintaining low pressure during long-term experiments.

After the 9-day pressure experiment, a small amount of gas was extracted from the MESCH and analyzed with the residual gas analyzer. The atmospheric composition was 99.1% CO_2, 0.5% O_2, and 0.3% H_2O. The quantities of O_2 and H_2O were close to the detection limit of the gas analyzer (~0.2%). The average O_2 leak rate into the MESCH was cal-

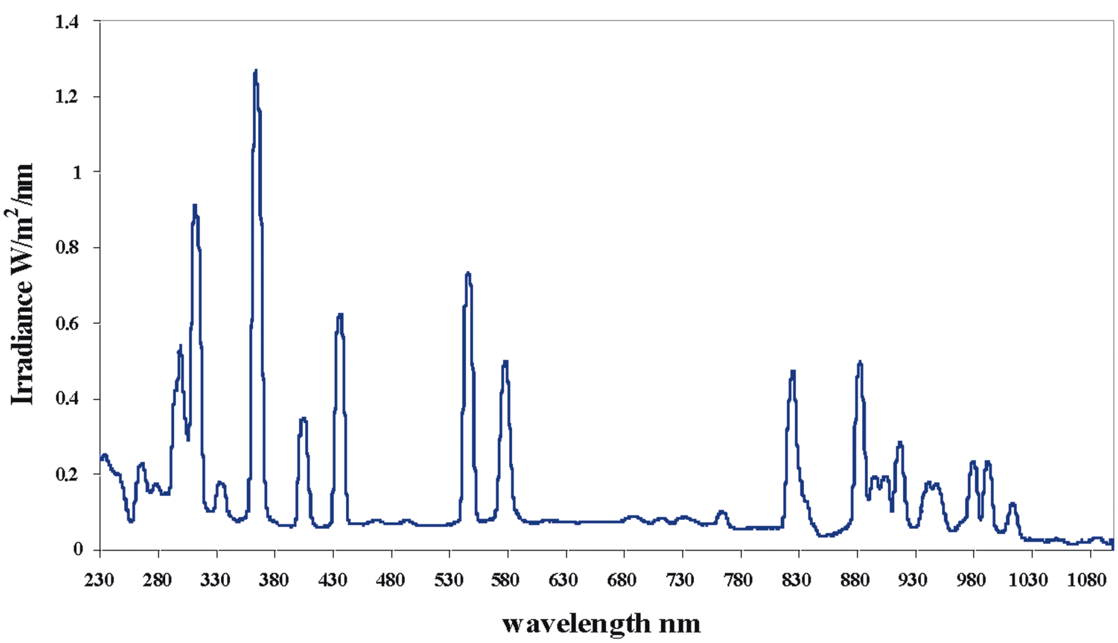

FIG. 3. A UV–near infrared irradiance spectrum taken inside the MESCH, at the sample during irradiation (with a lamp power of around 120 W).

culated by comparing the partial pressures of O_2 in the beginning and at the end of the test period. The O_2 leak rate was 0.004 mbar day^{-1}. Since the partial pressure of O_2 in the martian atmosphere is ~0.01 mbar, the MESCH atmosphere should be exchanged every 2–3 days when running O_2 sensitive experiments.

3.2. Sample and MESCH temperature

It has been our aim to reproduce the environmental conditions on Mars, specifically the near-surface region (*i.e.*, uppermost few cm), rather than to construct a chamber that has full (uniform) thermal control over a soil sample. When the surface of Mars is illuminated (heated) by the Sun, the surface temperature increases (exponentially) to a certain midday high; at depths below the surface, the temperature increase is slower (larger exponential time constant) and reaches a lower maximum temperature. This heating cycle is reproduced in the MESCH with the use of a cooled chamber that cools the sample and the application of heat with a lamp (solar simulator). The depth and time dependence of the sample temperature is not controlled in the MESCH; but, as on Mars, it is a function of the thermal properties of the soil materials (*e.g.*, heat capacity, thermal conductivity, thermal diffusivity). By varying the chamber temperature and the lamp power (heat), it is possible to vary the base soil sample temperature and the surface temperature increase, which are the 2 parameters of importance. The lowest measured chamber temperature yet achieved was −140°C, which is close to the minimum surface temperature of Mars (mid-winter, polar temperature).

Considering the low *in situ* temperatures in the martian regolith, we chose a temperature setting of the MESCH where the maximum temperature at the soil surface did not exceed −20°C in the absence of UV light. In the 9-day pressure experiment, a maximum temperature of −20°C was achieved at the sand surface in the dark by the following procedure:

The cooling mantle was flushed with liquid N_2 for 2 min, which resulted in a MESCH wall temperature of −69°C near the N_2 inlet. This was followed by a period of 7 min without N_2 flushing, which resulted in a temperature increase to −48°C (Fig. 4). Continuous repeated cycles of N_2 flushing resulted in a constant sample temperature of −25°C within 11–12 hours.

Cooling cycles were controlled as described above with a wall temperature setting of −50°C and a hysteresis of 2°C, which resulted in a mean MESCH wall temperature of −55.8°C. Due to minor differences in flow rates of the coolant, minor variations in the MESCH wall minimum temperature were observed when different liquid N_2 tanks were used. To minimize the variations in the minimum temperature, a flow meter was attached to the outlet of the cooling mantle, which enabled a more accurate control of the flow rate of liquid N_2.

In the absence of UV exposure of the soil sample, a minor variation of the sample temperature of ~4°C was observed in the MESCH, depending on the position of the sample in the carousel. The lowest temperature was measured in the carousel position right before the quartz glass window in the MESCH lid, and the highest temperature was measured in

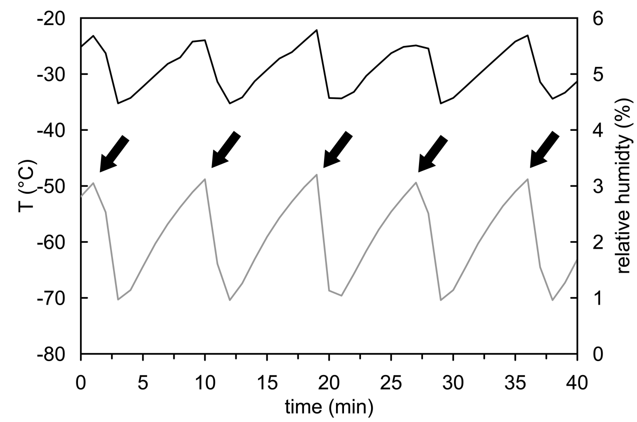

FIG. 4. The cyclic temperature variation inside the MESCH, measured near the N_2 inlet of the cooling mantle. The arrows indicate the beginning of a cooling cycle. The upper curve shows the relative humidity also measured near the N_2 inlet of the cooling mantle.

the position before the inspection window and the load-lock system. The observed temperature variation was probably caused by a restricted N_2 flow in the cooling mantle near the inspection window. This resulted in a slightly higher temperature on one side of the MESCH than on the other side. However, a temperature variation of ~4°C was negligible since the sample temperature never exceeded −20°C in the dark.

To determine the temperature increase of the soil as a function of depth and time after illumination by the lamp, a set of temperature measurements was performed at depths of 0 mm, 1 mm, 5 mm, 10 mm, and 15 mm below the surface of a fine-grained (95% of the particles less than 125 μm), freeze-dried permafrost soil sample from Svalbard. Thin (0.2 mm diameter) K-type thermocouple sensors were used, which were mounted horizontally from the sides of the sample holder. Two thermocouples were placed at positions equidistant from the walls and center of the sample holder. The temperature was monitored for at least 3 hours.

The UV solar simulation source emits light mostly in the optical and near infrared, as does the solar flux on Mars; this light is converted into heat on the soil sample surface. Prior to the studies of soil temperature rise, the heat produced by the lamp at the sample (lamp intensity, *I*) was quantified to be 273 W/m^2 by measuring the temperature increase of a known (coated) copper mass of the same dimension as the soil sample surface (40 mm diameter).

From simple thermodynamic arguments (ignoring the finite size of the sample holders), the temperature increase within the soil should fall linearly with depth, in this case down to a depth (d_b) of around 40 mm where the temperature increase becomes negligible. This temperature should be achieved (exponentially) after a time constant, which increases as the square of the depth, due to thermal diffusion within the soil samples. Based on these assumptions, it is possible to apply a semi-empirical formula to the soil temperature measurements, which can then be used to predict the temperature as a function of depth (d) and lamp exposure time (t) either from the lamp intensity

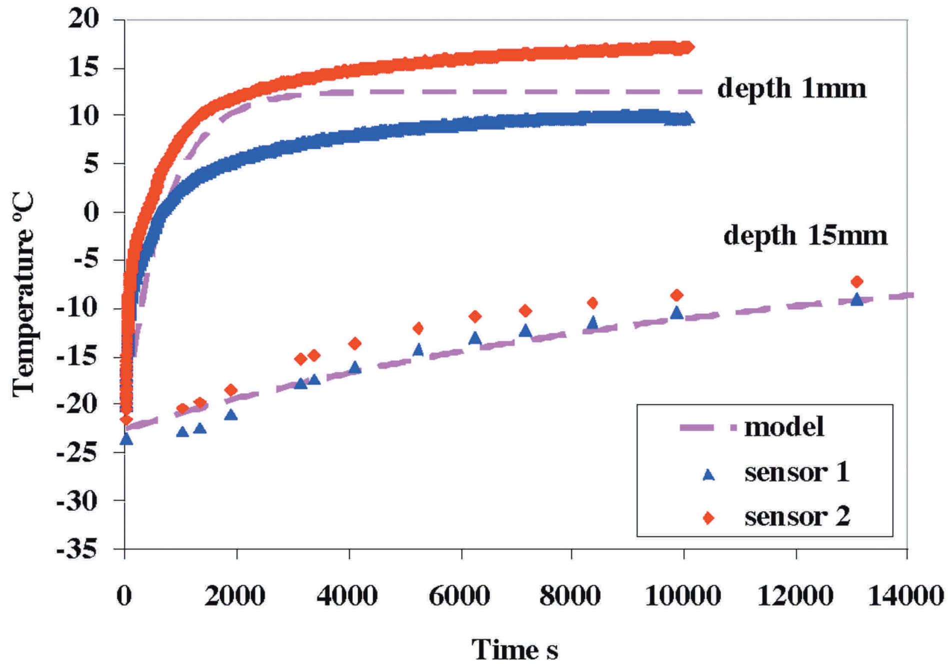

FIG. 5. The temperature of a permafrost soil sample measured using two thermocouples at different positions (sensor 1 and sensor 2) for two different depths: the upper curves are taken close to the surface of the sample (1 mm) and the lower curves are 15 mm below the surface. These measurements were taken within the MESCH (under martian conditions; specifically, around 9 mbar CO_2 atmosphere) after onset of irradiation exposure. The dashed lines are a theoretical fit (See Eq. 1).

(I) or from direct measurements of the surface temperature rise (dT_s).

$$T(d,t) = T_b + dT_s \times \frac{d_b - d}{d_b} \times \left[1 - \exp(-\frac{t}{kd^2 + \tau_s})\right] \quad (1)$$

where T_b is the deep soil temperature, dT_s is the soil surface temperature rise (after thermal stabilization), d_b is the deep-soil depth (empirically determined), k is the soil thermal diffusivity, and τ_s is the thermal time constant at the soil surface (measured). Based on the measurements made (using permafrost soil): $d_b = 37$ mm, $k = 46$ s/mm^2 and $\tau_s = 716$ s. With a measured lamp intensity of 273 W/m^2, a surface temperature increase of $dT_s = 33$°C was measured. Although dT_s may be measured directly, the surface temperature increase may also be estimated based on the lamp intensity (I); $dT_s = I \times \frac{33}{273}$.

Figure 5 shows the temperature increase for depths of 1 mm and 15 mm for both thermocouple sensors and the relevant fitting function (note the smaller temperature increase and longer equilibrium time at depth). As can be seen, there is significant variation in the output of the 2 thermocouple sensors, which is probably due to variation in light intensity across the surface. The semi-empirical function appears to reproduce the observations adequately within experimental uncertainty. Note that similar temperature measurements would be necessary for other types of soil, which would have different values for thermal diffusivity. Note also that only in long-term lamp exposure experiments, depending on the soil thermal properties, a stable temperature gradient within the soil sample would be established (see Eq. 1). These results demonstrate that heat generated by the UV solar simulation source affects the soil sample considerably deeper than the (direct) UV radiation does itself, as is the case on Mars. Ultraviolet radiation has been shown to penetrate mineral samples to a depth of only 20–82 μm (Schober and Lohmannsroben, 2000) and is expected to penetrate granular material to depths of the same order of magnitude as the grain size.

3.3. Humidity

Ice accretion was observed inside the MESCH on the wall adjacent to the N_2 inlet during cooling with liquid N_2. The ice sublimated before the onset of the next cooling cycle. To determine the cause for this cyclic pattern, the MESCH was evacuated to 10^{-3} mbar and sealed. Pressure changes were followed during 7 repeated cooling cycles. The pressure decreased by $\sim 4 \times 10^{-3}$ mbar during each cooling period and was followed by an increase in pressure during each period without cooling. Considering the temperature variation at the MESCH wall near the N_2 inlet, this observation indicated that H_2O was responsible for the cyclic pressure changes, though H_2O contributed $<0.1\%$ by volume to the atmosphere. Thus, the area close to the N_2 inlet, which is the coldest spot in the MESCH, traps residual moisture, which prevents the buildup of ice on the sample surfaces. Buildup of ice on samples in low-pressure chambers can be a problem if the samples are placed on a "cold finger" (ten Kate *et al.*, 2003).

4. Discussion

The approach taken in the design of this simulation chamber has been to reproduce the low-pressure (atmosphere) and low-temperature environment of Mars and to simulate the effect of solar flux with a xenon/mercury lamp, which may provide both (diurnal) heating and intense UVC. Based on the series of studies presented here, it can be seen that there are advantages and disadvantages with the current design. Specifically, with regard to humidity, applying cooling of the sample through the entire chamber cooling mantle ensures that the chamber walls (especially at the coolant inlet) are always significantly (more than 25°C) cooler than the sample. This has the effect of maintaining low humidity at the sample and avoiding surface water frost. Compared to cooling/heating of the sample directly (*e.g.,* with a cold finger), however, there is less thermal control of the sample. Also, although this system can ensure reasonable thermal stability, long cooling times (several hours) are required. There are also thermal gradients within the chamber such that sample rotating can cause temperature change. This could be avoided by way of improved thermal distribution, particularly between the sample holders and the chamber as well as across the chamber.

The use of a single UV/thermal lamp (effectively a solar simulator) reproduces the diurnal heating of a soil sample, though this is not independent of the UV exposure. It is desirable (for the envisioned biological experiments) that significantly greater UVC intensity (around 250 nm) is produced by the lamp such that effective exposure is maximized. The use of filters or a combination of lamps (optical/IR/UV) could provide a more realistic or controllable heat/UV source. It should be stressed that the current light source provides reasonable diurnal surface temperature increase and fulfils the desire to perform large UVC doses (months/years on Mars) within reasonable simulation run time (days/weeks).

5. Conclusion

Our MESCH facility allows for the simulation of the following martian conditions: temperature, UV radiation, atmospheric pressure, and gas composition. The computer-controlled liquid N_2 flow-through cooling system provides effective temperature control. The design of the cooling system prevents formation of ice on the samples, which can be a problem when cold-finger–type devices are used. Environmental data from the MESCH are logged on a computer, which uses these data to control temperature and sample UV exposure. Thermocouple measurements in combination with mathematical modeling allow the reconstruction of the temperature profiles of individual samples.

The MESCH is suitable for the exposure of multiple samples in each experiment and can be used for the incubation of different sample types: microbial communities, pure cultures, and biomolecules. Survival studies are not restricted to the exposure to UV, since other radiation devices can be used in combination with the MESCH. For instance, simulation of Earth orbit could be achieved by creating a vacuum in the MESCH and by radiating with UV and ionizing radiation.

Thus, the MESCH is not restricted to simulations of the martian environment but can be used for a whole range of experiments that require incubation of any type of sample in an environment with a controlled atmospheric composition, temperature, and radiation flux.

6. Acknowledgments

This research was supported by the Danish National Science Research Council grant 21-03-0557, and L.L.J. was partly financed by Oticon. The authors wish to thank Henrik Bechtold, Uffe Simonsen, Einer Larsen, and Poul Erik Mikkelsen for excellent technical skills during the construction of the MESCH and for advice and assistance during the testing and evaluation phase. Thanks to professor Peter Ogilby for help with the UV source.

Abbreviations

IR, infrared light; MESCH, Mars Environmental Simulation Chamber; UV, ultraviolet; VIS, visible light.

References

Belikova, E.V., Komolova, G.S., and Egorov I.A. (1968) Effect of a simulated martian environment on certain enzymes. *Environmental Space Sciences* 2:426–430.

Brack, A. (2000) The exobiology exploration of Mars: a survey of the European approaches. *Planet. Space Sci.* 48:1023–1026.

Bullock, M.A., Moore, J.M., and Mellon, M.T. (2004) Laboratory simulations of Mars aqueous geochemistry. *Icarus* 170: 404–423.

Bunce, N.J. (1987) Actinometry. In *CRC Handbook of Organic Photochemistry,* Vol.1, edited by J.C. Scaiano, CRC Press, Boca Raton, FL, pp 241–244.

Cockell, C.S., Schuerger, A.C., Billi, D., Friedmann, E.I., and Panitz, C. (2005) Effects of a simulated martian UV flux on the cyanobacterium, *Chroococcidiopsis* sp. 029. *Astrobiology* 5: 127–140.

Davis, I. and Fulton, J.D. (1959) Microbiologic studies on ecologic considerations of the martian environment. *Aeromed. Rev.* 2-60:1–10.

Diaz, B. and Schulze-Makuch, D. (2006) Microbial survival rates of *Escherichia coli* and *Deiniococcus radiodurans* under low temperature, low pressure, amd UV irradiation conditions, and their relevance to possible martian life. *Astrobiology* 6:332–347.

Foster, T.L. and Winans, L. (1974) Effect of a simulated martian environment on growth of selected microorganisms. *Tex. Rep. Biol. Med.* 32:608–609.

Foster, T.L., Winans, L., Casey, R.C., Jr., and Kirschner, L.E. (1978) Response of terrestrial microorganisms to a simulated martian environment. *Appl. Environ. Microbiol.* 35:730–737.

Fraser, H.J. and van Dishoeck, E.F. (2003) SURFRESIDE: a novel experiment to study surface chemistry under interstellar and protostellar conditions. *Adv. Space Res.* 33:14–22.

Fulton, J.D. (1958) Survival of terrestrial microorganisms under simulated martian conditions. In *Physics and Medicine of the Atmosphere and Space,* edited by O.O. Benson and H. Strughold, John Wiley & Sons, New York, pp 606–613.

Galletta, G., Ferri, F., Fanti, G., D'Alessandro, M., Bertoloni, G., Pavarin, D., Bettanini, C., Cozza, P., Pretto, P., Bianchini, G., and Debi, S. (2006) S.A.M., the Italian Martian Simulation Chamber. *Orig. Life Evol. Biosph.* 36:625–627.

Gontareva, N.B. (2005) Photochemical stability of biomolecules in the experiments modelling martian surface conditions. *Int. J. Astrobiology* 4:93–96.

Green, R.H., Taylor, D.M., Gustan, E.A., Fraser, S.J., and Olson, R.L. (1971) Survival of microorganisms in a simulated martian environment. *Space Life Sci.* 3:12–24.

Hagen, C.A., Ehrlich R., and Hawrylewicz E. (1964) Survival of microorganisms in simulated martian environment. 1. *Bacillus subtilis* var. *globigii*. *Appl. Microbiol.* 12:215–218.

Hagen, C.A., Hawrylewicz, E., and Ehrlich, R. (1967) Survival of microorganisms in a simulated martian environment. 2. Moisture and oxygen requirements for germination of *Bacillus cereus* and *Bacillus subtilis* var. *niger* spores. *Appl. Microbiol.* 15:285–291.

Hagen, C.A., Hawrylewicz, E.J., Anderson, B.T., and Cephus, M.L. (1970) Effect of ultraviolet on the survival of bacteria airborne in simulated martian dust clouds. *Life Sci. Space Res.* 8:53–58.

Hansen, A.A., Merrison, J., Nørnberg, P., Lomstein, B.A., and Finster, K. (2005) Activity and stability of a complex bacterial soil community under simulated martian conditions. *Int. J. Astrobiology* 4:135–144.

Hawrylewicz, E., Gowdy, B., and Ehrlich, R. (1962) Microorganisms under a simulated martian environment. *Nature* 193:497.

Hawrylewicz, E.J., Hagen, C.A., and Ehrlich, R. (1965) Response of microorganisms to a simulated martian environment. *Life Sci. Space Res.* 3:64–73.

Hawrylewicz, E.J., Hagen, C.A., Tolkacz, V., Anderson, B.T., and Ewing, M. (1968) Probability of growth (p_G) of viable microorganisms in martian environments. *Life Sci. Space Res.* 6:146–156.

Hubbard, J.S., Hardy, J.P., and Horowitz, N.H. (1971) Photocatalytic production of organic compounds from CO and H_2O in a simulated martian atmosphere. *Proc. Natl. Acad. Sci. U.S.A.* 68:574–580.

Imshenetsky, A.A., Abyzov, S.S., Voronov, G.T., Kuzjurina, L.A., Lysenko, S.V., Sotnikov, G.G., and Fedorova, R.I. (1967) Exobiology and the effect of physical factors on micro-organisms. *Life Sci. Space Res.* 5:250–260.

Imshenetsky, A.A., Kouzyurina, L.A., and Jakshina, V.M. (1973) On the multiplication of xerophilic micro-organisms under simulated martian conditions. *Life Sci. Space Res.* 11:63–66.

Imshenetskii, A.A., Murzakov, B.G., Evdokimova, M.D., and Dorofeeva, I.K. (1984) Survival of bacteria in the artificial Mars apparatus. *Microbiology* 53:594–600.

Kieffer, H.H., Jakosky, B.M., Snyder, C.W., and Matthews, M.S. (1992) *Mars: Space Science Series*, The University of Arizona Press, Tucson, AZ.

Koike, J., Oshima, T., Kobayashi, K., and Kawasaki, Y. (1995) Studies in the search for life on Mars. *Adv. Space Res.* 15:211–214.

Koike, J., Hori, T., Katahira, Y., Koike, K.A., Tanaka, K., Kobayashi, K., and Kawasaki, Y. (1996) Fundamental studies concerning planetary quarantine in space. *Adv. Space Res.* 18:339–344.

Kolb, C., Abart, R., Bérces, A., Cockell, C., Garry, J.R.C., Hansen, A.A., Hohenau, W., Kargl, G., Lammer, H., Patel, M.R., Rettberg, P., and Stan-Lotter, H. (2005) A UV simulator for the incident martian surface radiation and its applications. *Int. J. Astrobiology* 4:241–249.

Kooistra, J.A., Mitchell R.B., and Strughold, H. (1958) The behavior of microorganisms under simulated martian environmental conditions. *Publ. Astron. Soc. Pac.* 70:64–69.

Lobitz, B., Wood, B.L., Averner, M.M., and McKay, C.P. (2001) Use of spacecraft data to derive regions on Mars where liquid water would be stable. *Proc. Natl. Acad. Sci. U.S.A.* 98:2132–2137.

Lozina-Lozinsky, L.K. and Bychenkova, V.N. (1969) Resistance of the protozoan *Colpoda maupasi* to martian conditions of atmospheric pressure and low partial pressure of oxygen. *Life Sci. Space Res.* 7:149–155.

Lozina-Lozinsky, L.K., Bychenkova, V.N., Zaar, E.I., Levin, V.L., and Rumyantseva, V.M. (1971) Some potentialities of living organisms under simulated martian conditions. *Life Sci. Space Res.* 9:159–165.

Mancinelli, R.L. and Klovstad, M. (2000) Martian soil and UV radiation: microbial viability assessment on spacecraft surfaces. *Planet. Space Sci.* 48:1093–1097.

Mateo-Martí, E., Prieto-Ballesteros, O., Sobrado, J.M., Gómez-Elvira, J., and Martín-Gago, J.A. (2006) A chamber for studying planetary environments and its applications to astrobiology. *Measurements Science and Technology* 17:2274–2280.

McDonald, G.D., de Vanssay, E., and Buckley, J.R. (1998) Oxidation of organic macromolecules by hydrogen peroxide: implications for stability of biomarkers on Mars. *Icarus* 132:170–175.

Merrison, J., Jensen, J., Kinch, K., Mugford, R., and Nornberg, P. (2004) The electrical properties of Mars analogue dust. *Planet. Space Sci.* 52:279–290.

Moll, D.M. and Vestal, J.R. (1992) Survival of microorganisms in smectite clays: implications for martian exobiology. *Icarus* 98:233–239.

Moore, J.M. and Bullock, M.-A. (1999) Experimental studies of Mars-analog brines. *J. Geophys. Res.* 104:21925–21934.

Moore, J.M. and Sears, D.W.G. (2006) On laboratory simulation and the effect of small temperature dependence oscillations about the freezing point and ice formation on the evaporation rate of water on Mars. *Astrobiology* 6:644–650.

Morozova, D., Möhlmann, D., and Wagner, D. (2006) Survival of methanogenic archaea from Siberian permafrost under simulated martian thermal conditions. *Orig. Life Evol. Biosph.* 37, 189–200.

Nicholson, W.L. and Schuerger A.C. (2005) *Bacillus subtilis* spore survival and expression of germination-induced bioluminescence after prolonged incubation under simulated Mars atmospheric pressure and composition: implications for planetary protection and lithopanspermia. *Astrobiology* 5:536–544.

Oro, J. and Holzer, G. (1979) Photolytic degradation and oxidation of organic compounds under simulated martian conditions. *J. Mol. Evol.* 14:153–160.

Packer, E., Scher, S., and Sagan, C. (1963) Biological contamination of Mars. 2. Cold and aridity as constraints on the survival of terrestrial microorganisms in simulated martian environments. *Icarus* 2:293–316.

Patel, M.R., Christou, A.A., Cockell, C.S., Ringrose, T.J., and Zarnecki, J.C. (2004) The UV environment of the Beagle 2 landing site: detailed investigations and detection of atmospheric state. *Icarus* 168:93–115.

Rannou, P., Chassefière, E., Encrenaz, T., Erard, S., Génin, J.M., Imgrin, J., Jambon, A., Jolivet, J.P., Raulin, F., Renault, P., Rochette, P., Person, A., Siguier, J.M., and Toublanc, D. (2001) EXOCAM: Mars in a box to simulate soil-atmosphere interactions. *Adv. Space Res.* 27:189–193.

Schober, L. and Lohmannsroben, H.G. (2000) Determination of optical parameters for light penetration in particulate materials and soils with diffuse reflectance (DR) spectroscopy. *J. Environ. Monit.* 2:651–655.

Schuerger, A.C. and Nicholson, W.L. (2006) Interactive effects of hypobaria, low temperature, and CO_2 atmosphere inhibit the growth of mesophilic *Bacillus* spp. under simulated martian conditions. *Icarus* 185:143–152.

Schuerger, A.C., Mancinelli, R.L., Kern, R.G., Rothschild, L.J., and McKay, C.P. (2003) Survival of endospores of *Bacillus subtilis* on spacecraft surfaces under simulated martian environments: implications for the forward contamination of Mars. *Icarus* 165:253–276.

Schuerger, A.C., Richards, J.T., Hintze, P.E., and Kern, R.G. (2005) Surface characteristics of spacecraft components affect the aggregation of microorganisms and may lead to different survival rates of bacteria on Mars landers. *Astrobiology* 5:545–559.

Schuerger, A.C., Richards, J.T., Newcombe, D.A., and Venkateswaran, K. (2006) Rapid inactivation of seven *Bacillus* spp. under simulated Mars UV irradiation. *Icarus* 181:52–62.

Sears, D.W.G., Benoit, P.H., McKeever, S.W.S., Banerjee, D., Kral, T., Stites, W., Roe, L., Jansma, P., and Mattioli, G. (2002) Investigation of biological, chemical and physical processes on and in planetary surfaces by laboratory simulation. *Planet. Space Sci.* 50:821–828.

Seidensticker, K.J., Kochan, H., and Möhlmann, D. (1995) The DLR small simulation chamber: a tool for cometary research in the lab. *Adv. Space Res.* 10:29–34.

Squyres, S.W., Arvidson, R.E., Bell, J.F., Bruckner, J., Cabrol, N.A., Calvin, W., Carr, M.H., Christensen, P.R., Clark, B.C., Crumpler, L., Des Marais, D.J., d'Uston, C., Economou, T., Farmer, J., Farrand, W., Folkner, W., Golombek, M., Gorevan, S., Grant, J.A., Greeley, R., Grotzinger, J., Haskin, L., Herkenhoff, K.E., Hviid, S., Johnson, J., Klingelhofer, G., Knoll, A., Landis, G., Lemmon, M., Li, R., Madsen, M.B., Malin, M.C., McLennan, S.M., McSween, H.Y., Ming, D.W., Moersch, J., Morris, R.V., Parker, T., Rice, J.W., Richter, L., Rieder, R., Sims, M., Smith, M., Smith, P., Soderblom, L.A., Sullivan, R., Wanke, H., Wdowiak, T., Wolff, M., and Yen, A. (2004a) The Spirit Rover's Athena science investigation at Gusev Crater, Mars. *Science* 305:794–799.

Squyres, S.W., Arvidson, R.E., Bell, J.F., Bruckner, J., Cabrol, N.A., Calvin, W., Carr, M.H., Christensen, P.R., Clark, B.C., Crumpter, L., Des Marais, D.J., d'Uston, C., Economou, T., Farmer, J., Farrand, W., Folkner, W., Golombek, M., Gorevan, S., Grant, J.A., Greeley, R., Grotzinger, J., Haskin, L., Herkenhoff, K.E., Hviid, S., Johnson, J., Klingelhofer, G., Knoll, A.H., Landis, G., Lemmon, M., Li, R., Madsen, M.B., Malin, M.C., McLennan, S.M., McSween, H.Y., Ming, D.W., Moersch, J., Morris, R.V., Parker, T., Rice, J.W., Richter, L., Rieder, R., Sims, M., Smith, M., Smith, P., Soderblom, L.A., Sullivan, R., Wanke, H., Wdowiak, T., Wolff, M., and Yen, A. (2004b) The Opportunity Rover's Athena science investigation at Meridiani Planum, Mars. *Science* 306:1698–1703.

Stan-Lotter, H., Radax, C., Gruber, C., Legat, A., Pfaffenhuemer, M., Wieland, H., Leuko, S., Weidler, G., Kömle, N., and Kargl, G. (2003) Astrobiology with haloarchaea from Permo-Triassic rock salt. *Int. J. Astrobiology* 4:271–284.

Stoker, C.R. and Bullock, M.A. (1997) Organic degradation under simulated martian conditions. *J. Geophys. Res.* 102: 10881–10888.

Tauscher, C., Schuerger, A.C., and Nicholson W.L. (2006) Survival and germinability of *Bacillus subtilis* spores exposed to simulated Mars solar radiation: implications for life detection and planetray protection. *Astrobiology* 6:592–605.

ten Kate, I.L., Ruiterkamp, R., Botta, O., Lehmann, B., Gomez Hernandez, C., Boudin, N., Foing, B.H., and Ehrenfreund, P. (2003) Investigating complex organic compounds in a simulated Mars environment. *Int. J. Astrobiology* 1:387–399.

ten Kate, I.L., Garry, J.R.C., Peeters, Z., Quinn, R., Foing, B., and Ehrenfreund, P. (2005) Amino acid photostability on the martian surface. *Meteorit. Planet. Sci.* 40:1185–1193.

ten Kate, I.L., Garry, J.R.C., Peeters, Z., Foing, B., and Ehrenfreund, P. (2006) The effect of martian near surface conditions on the photochemistry of amino acids. *Planet. Space Sci.* 54:296–302.

UALPL, The University of Arizona Lunar and Planetary Laboratory. (2008) *Phoenix Mars Mission,* University of Arizona, Tuscon, http://phoenix.lpl.arizona.edu.

Young, R.S., Deal, P., Bell, J., and Allen, J. (1963) Effect of diurnal freeze-thawing on survival and growth of selected bacteria. *Nature* 199:1078–1079.

Zhukova, A.I. and Kondratyev, I.I. (1965) On artificial martian conditions reproduced for microbiological research. *Life Sci. Space Res.* 3:120–126.

Zill, L.P., Mack, R., and Devincenzi, D.L. (1979) Mars ultrviolet simulation facility. *J. Mol. Evol.* 6:79–89.

Address reprint requests to:
Kai Finster
Department of Biological Sciences
Section for Microbiology
University of Aarhus
Ny Munkegade, Bld. 1540
DK-8000 Aarhus C, Denmark

E-mail: kai.finster@biology.au.dk